Supporting Information

Biodegradable Persistent ROS-Generating Nanosonosensitizers for Enhanced Synergistic Cancer Therapy by Inducing Cascaded Oxidative Stress

Yue Chen[a†], Tong Ding[b†], Zhengzheng Qian[a†], Zerui Ma[a], Liming Zhou[a], Zhiling Li[b], Runkai Lv[c], Yinghui Xu[a], Yingjie Xu[a], Linhui Hao[c], Chen Zhu[d], Xikuang Yao[c]*, Wenying Yu[b]*, and Wenpei Fan[a]**

[a]*State Key Laboratory of Natural Medicines and Jiangsu Key Laboratory of Drug Discovery for Metabolic Diseases, Center of Advanced Pharmaceuticals and Biomaterials, China Pharmaceutical University, Nanjing 211198, China.*

[b]*Jiangsu Key Laboratory of Bioactive Natural Product Research and State Key Laboratory of Natural Medicines, China Pharmaceutical University, Nanjing 211100, China*

[c]*School of Flexible Electronics (Future Technologies) and Institute of Advanced Materials (IAM), Nanjing Tech University (Nanjing Tech), Nanjing 211816, China*

[d]*Department of Orthopedics, The First Affiliated Hospital of USTC, Division of Life Sciences and Medicine, University of Science and Technology of China, Hefei 230001, China*

**Corresponding Author(s): Wenpei Fan (E-mail address: wenpei.fan@cpu.edu.cn); Wenying Yu (E-mail address: ywy@cpu.edu.cn); Xikuang Yao (E-mail address: iamxyao@njtech.edu.cn); Chen Zhu (E-mail address: zhuchena@ustc.edu.cn)*

†*Yue Chen, Tong Ding and Zhengzheng Qian contributed equally to this work.*

Experimental Section

ROS generation from CaO_2@PCN

The Temp was added to the CaO_2@PCN solution (pH 5.5). Then the mixture was treated with US irradiation (2.0 W/cm^2, 3 MHz, and 50% duty cycle) for 5 min and then transferred to the quantitative capillary and measured by electron paramagnetic resonance spectrometer (Bruker A200, Germany). For comparison, the PBS (pH 5.5) and CaO_2@PCN solutions (pH 5.5) without US irradiation were detected under the same conditions.

The DPBF solution was mixed with the CaO_2@PCN solution (pH 5.5). After US irradiation durations (2.0 W/cm^2, 3 MHz, and 50% duty cycle), the absorbance of DPBF at 420 nm was recorded to quantify the generation rate of $^1O_2$ within 3 min. For comparison, the CaO_2@PCN solution without US irradiation was detected under the same conditions.

***In vitro* cytotoxicity evaluation**

First, to investigate the cell toxicities of different nanoformulations, 4T1 cells were seeded in 96-well plates, each containing 5×10^3 cells, and cultured at 37℃ with 5% CO_2 for 12 h. Then, the original culture media were removed and the cells were washed thrice with PBS. Then, the cells were subjected to four different nanoformulations at various concentrations in RPMI 1640 media and incubated for 24 h: (1) CaO_2 (10, 20, 30, 40, 50, 60, 80, 90, 100, 120, and 140 μg/mL); (2) PCN (20, 40, 60, 120, 180, 240, 300, 360, 420, 480, and 600 μg/mL); and (3) CaO_2@PCN (0, 10, 20, 30, 40, 50, 75, 100, 130 and 200 μg/mL). Next, 20 μL of MTT solution (5 mg/mL) was added to each well. After 4 h of incubation, the MTT solution in each well was replaced with 150 μL of DMSO to dissolve crystals. Finally, the absorbance of each well was measured at 490 nm using a microplate reader. The cell viability was calculated according to the following formula: cell viability (%) = (OD_{sample}-OD_{blank})/($OD_{control}$-OD_{blank}) × 100.

Second, to investigate the cell toxicities of PCN or CaO_2@PCN upon US irradiation, 4T1 cells were seeded in 96-well plates at a density of 5×10^3 per well and cultured at 37℃ with 5% CO_2 for 12 h. Afterward, the original culture media were removed and different concentrations of PCN or CaO_2@PCN (TCPP = 0, 1.25, 2.50, 5.00, 7.50, and 10.00 μg/mL) were added to each well for another 12 h of incubation. Then, these cells were subjected to varied power densities of US irradiation (3 MHz, and 50% duty cycle) for 5 min and cultured for another 24 h. After that, 20 μL of MTT was added, following 4 h of co-incubation. Subsequently, the culture media containing MTT was removed and 150 μL of DMSO was added to dissolve

crystals. Finally, the absorbance of each well was tested by a microplate reader at a wavelength of 490 nm.

Detection of intracellular ROS production

4T1 cells were seeded in a 12-well plate at a density of 1.5×10^5 per well and cultured for 12 h at 37℃. Subsequently, the old culture was replaced with a fresh one containing RPMI 1640 media (control), 87.2 μg/mL PCN ([TCPP] = 10 μg/mL), or 75 μg/mL CaO_2@PCN ([TCPP] = 10 μg/mL, $[Ca^{2+}]$ = 23 μg/mL) for 12 h of co-incubation. Afterward, the cells were subjected to US irradiation (2.0 W/cm^2, 3 MHz, and 50% duty cycle) and cultured for another 24 hours. To study the effect of US power densities on ROS generation, the 4T1 cells cultured with CaO_2@PCN ([TCPP] = 10 μg/mL, $[Ca^{2+}]$ = 23 μg/mL) were treated with the different power densities of US irradiation. Next, after washing with PBS several times, the cells were stained with DCFH-DA solution (10 μM) for 30 min. Finally, the intracellular ROS was observed by CLSM and analyzed by flow cytometry.

4T1 cells were seeded in a 12-well plate at a density of 1.5×10^5 per well and cultured for 12 h at 37℃. Subsequently, the old culture was replaced with a fresh one containing 75 μg/mL CaO_2@PCN ([TCPP] = 10 μg/mL, $[Ca^{2+}]$ = 23 μg/mL) for 12 h of co-incubation. Afterwards, the cells were subjected to different densities of the US irradiation (3 MHz, and 50% duty cycle) and cultured for another 24 h. Next, after washing with PBS several times, the cells were stained with DCFH-DA solution (10 μM) for 30 min. Finally, the intracellular ROS was observed by CLSM and analyzed by flow cytometry.

***In vivo* pharmacokinetics**

The CaO_2@PCN solution at a dose of 18 mg/kg was intravenously injected into balb/c mice. Then, 300 μL of blood was collected from the orbital vein at 10 min, 30 min, 1 h, 2 h, 4 h, 8 h, 12 h, 24 h, and 48 h, and the TCPP concentration in plasma was determined by a microplate reader. Data were analyzed by regression analysis using biexponential decay functions.

Hemolysis test

Red blood cells (RBC) were isolated from the fresh blood of mice by centrifugation at 3000 rpm for 15 min. The cells were purified by rinsing with saline several times until the supernatant cleared up. Then, the suspension of RBCs was diluted with 2 mL of saline. Next, 0.1 mL of the above solution was added into 0.9 mL of water (positive control), saline (negative control), or saline containing CaO_2, PCN, and CaO_2@PCN. After incubating at 37℃ for 2 h, the OD at 540 nm of the collected supernatant was

measured. The percentage of hemolysis was calculated using the following equation: Hemolysis (%) = $(OD_{sample}- OD_{negative})/ (OD_{positive}- OD_{negative}) \times 100$.

Supplemental Figures

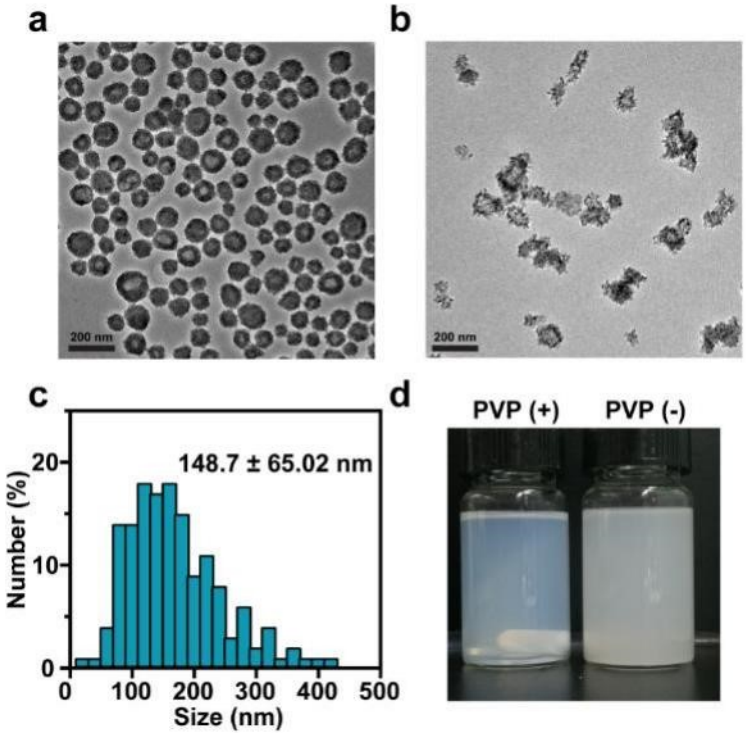

Figure S1. (a, b). TEM images of CaO_2 were prepared in the (a) presence and (b) absence of PVP. (c). Particle size distribution of CaO_2 prepared in the absence of PVP. (d). Photographs of ethanol solution of CaO_2 prepared in the presence (left) and absence (right) of PVP. Scale bar, 200 nm.

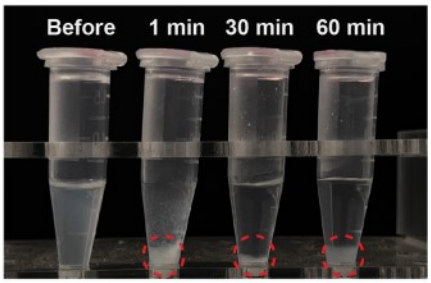

Figure S2. The photograph of CaO_2 after different times of incubation under pH 7.4.

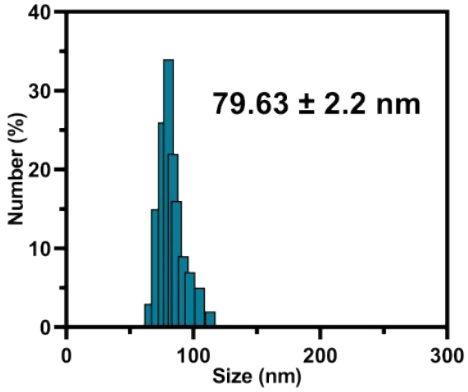

Figure S3. Particle size distribution of CaO_2@PCN prepared by 5 mg/mL CaO_2 (prepared by 12 mM $CaCl_2$) and 0.0625 mg/mL TCPP.

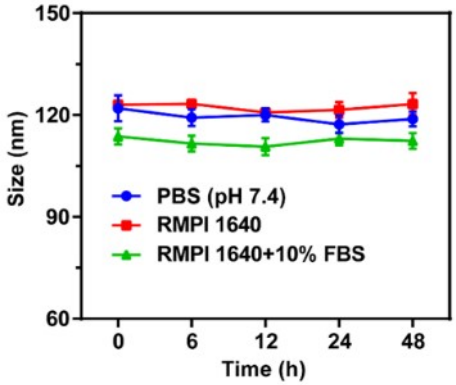

Figure S4. Hydrodynamic size changes of CaO_2@PCN after varied times of incubation in PBS (pH 7.4), RMPI 1640, and RMPI 1640 with 10% fetal bovine serum. Data were expressed as mean ± SD (n = 3).

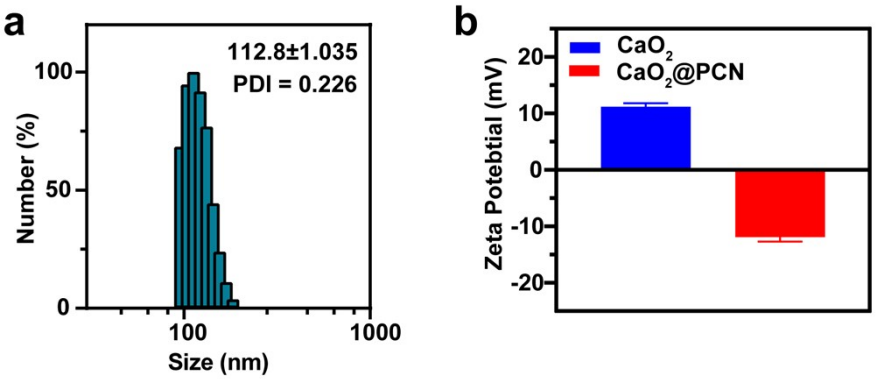

Figure S5. Hydrodynamic size (a) and Zeta potential (b) of CaO_2@PCN. Data were expressed as mean ± SD (n = 3).

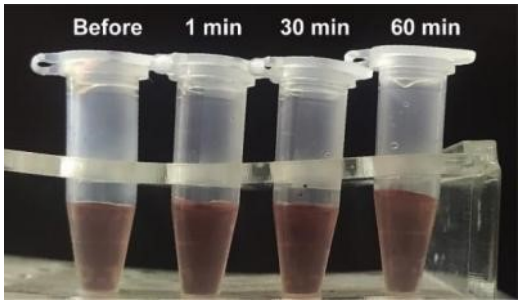

Figure S6. The photograph of CaO_2@PCN after different times of incubation under pH 7.4.

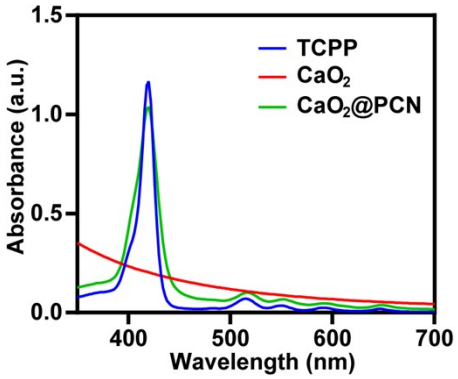

Figure S7. UV-Vis absorption spectra of free TCPP, CaO_2, and CaO_2@PCN nanoparticles.

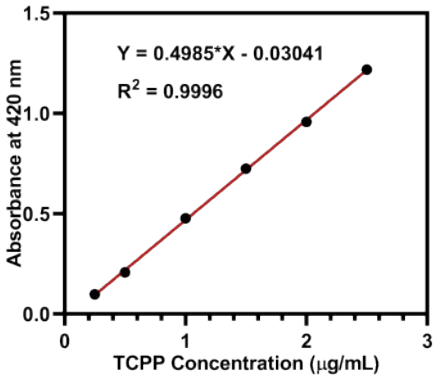

Figure S8. The standard calibration curve of free TCPP based on its absorbance at 420 nm.

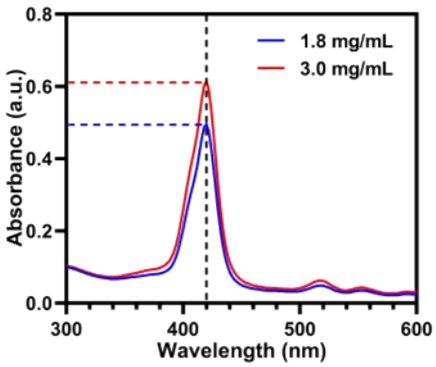

Figure S9. UV-Vis absorption spectra of different CaO_2@PCN concentrations.

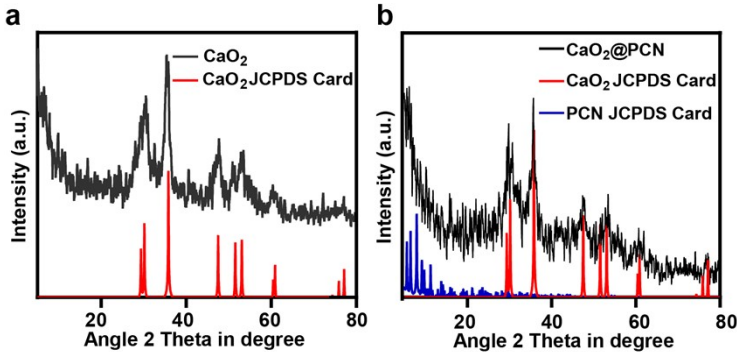

Figure S10. XRD patterns of (a) CaO_2 and (b) CaO_2@PCN.

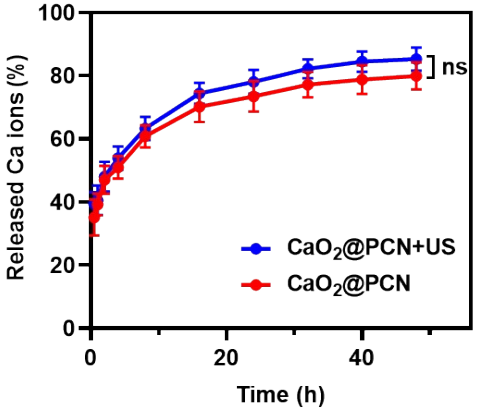

Figure S11. Time-dependent release profiles of Ca^{2+} from CaO_2@PCN with or without the US treatment. Data were expressed as mean ± SD (n = 3). ns, no significance.

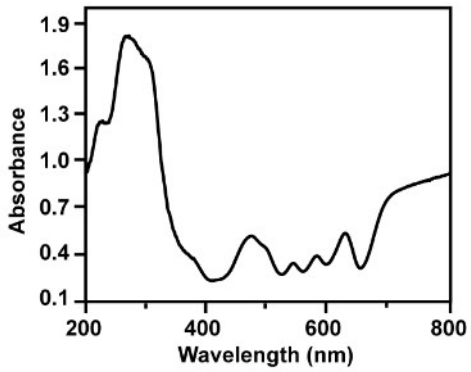

Figure S12. UV-Vis diffuse reflectance spectroscopy spectra of CaO_2@PCN.

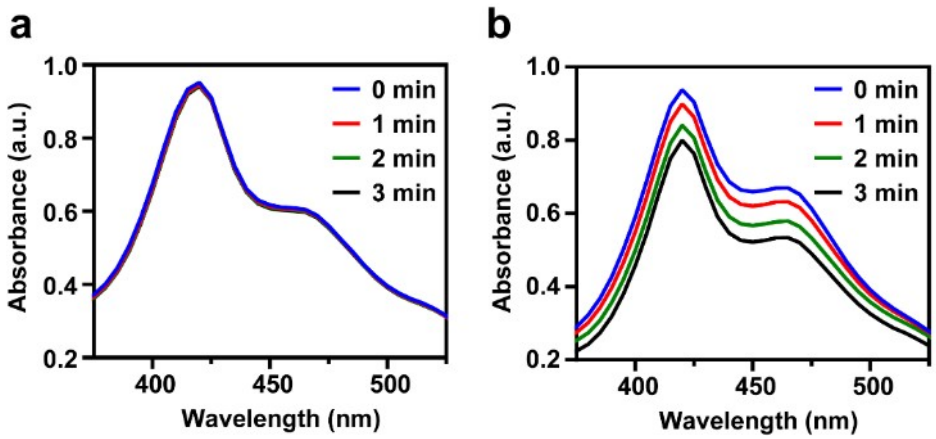

Figure S13. Time-dependent oxidation of DPBF as an indicator of $^1O_2$ generation arising from CaO_2@PCN without (a) and with (b) the US irradiation.

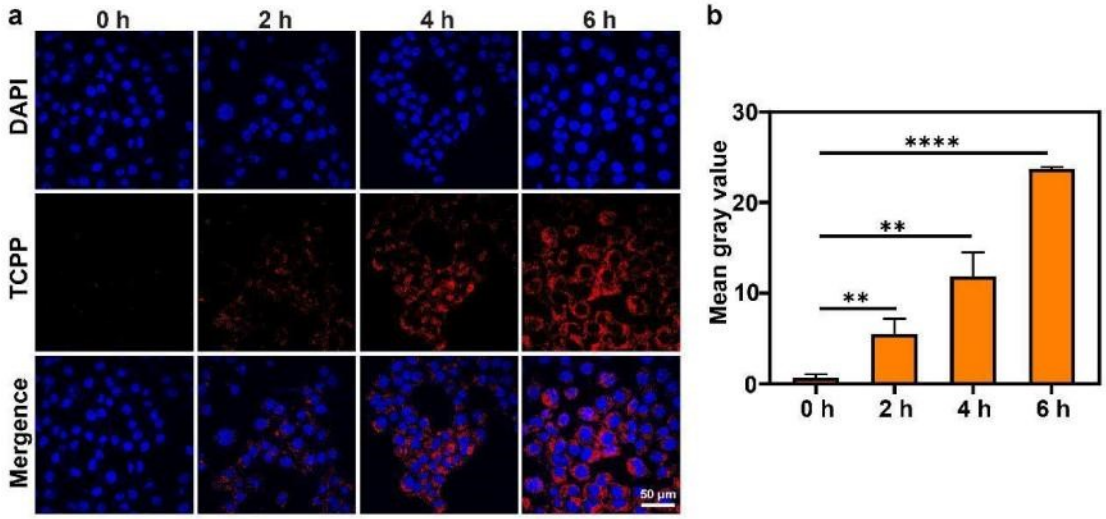

Figure S14. (a) CLSM images (red, TCPP; blue, DAPI) and (b) quantitative analyses of cellular uptake of 4T1 cells after incubation with CaO_2@PCN for 0, 2, 4, and 6 h. Data were expressed as mean ± SD (n = 3). ***P* < 0.01, *****P* < 0.0001. Scale bar, 50 μm.

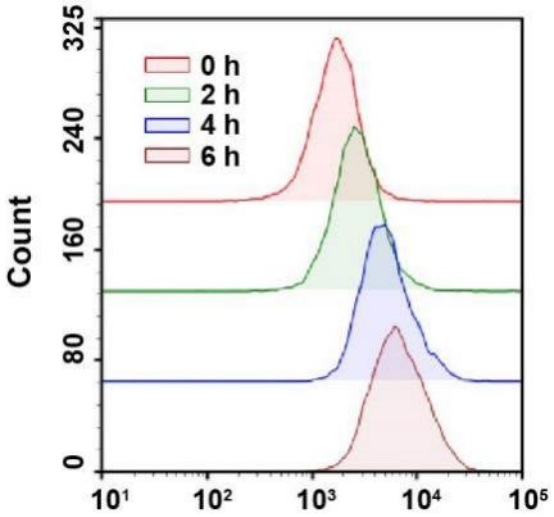

Figure S15. Flow cytometry analysis of cellular uptake of 4T1 cells after incubation with CaO_2@PCN for 0, 2, 4, and 6 h.

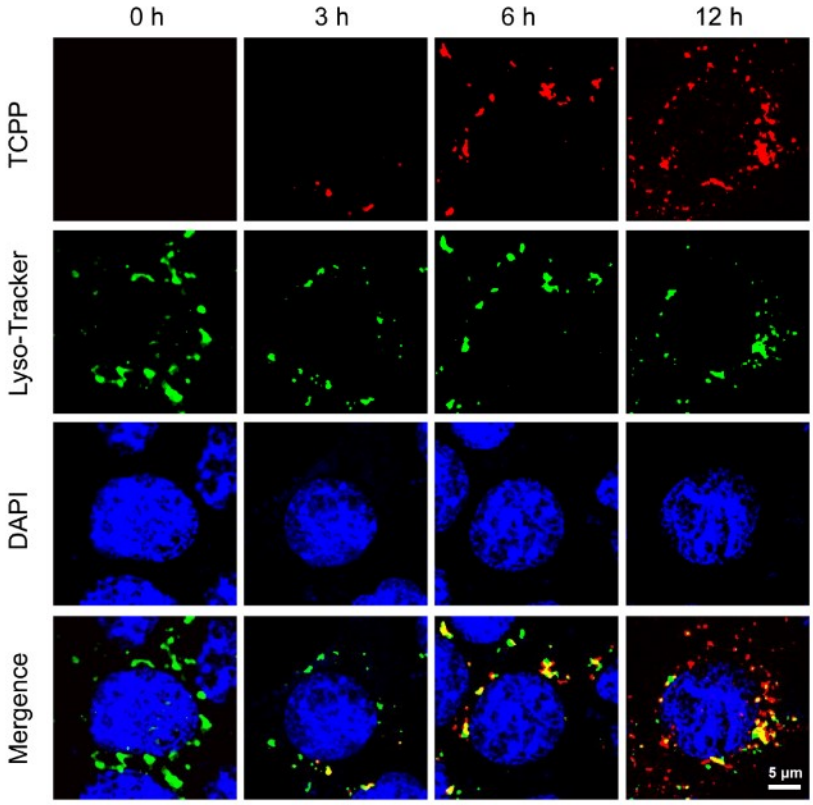

Figure S16. CLSM images of the distribution of TCPP in the lysosome of 4T1 cells after incubation with CaO2@PCN for 0, 3, 6, and 12 h. Scale bar, 5 μm.

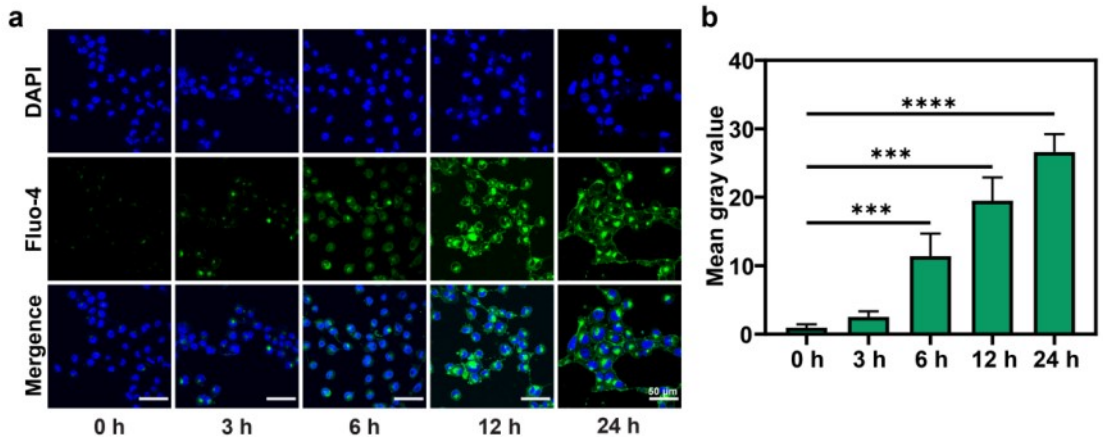

Figure S17. CLSM images (green, Fluo-4; blue, DAPI) and (b) quantitative analyses of intracellular Ca^{2+} level in 4T1 cells after incubation with CaO_2@PCN for 0, 3, 6, 12, and 24 h. Data were expressed as mean ± SD (n = 3). ***P < 0.001, ****P < 0.0001. Scale bar, 50 μm.

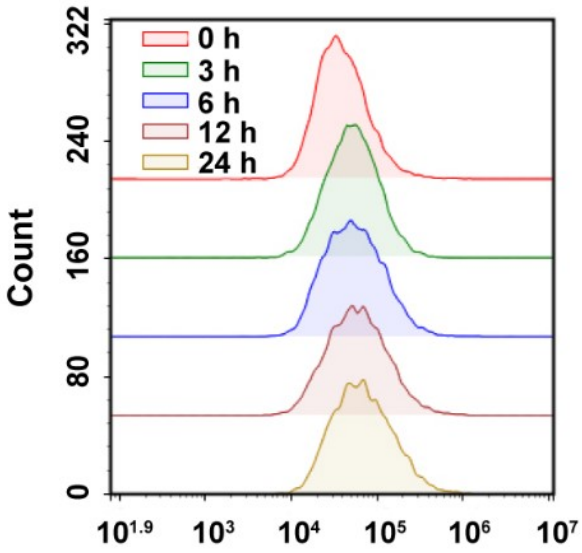

Figure S18. Flow cytometry analysis of intracellular Ca^{2+} in 4T1 cells after incubation with CaO_2@PCN for 0, 3, 6, 12, and 24 h.

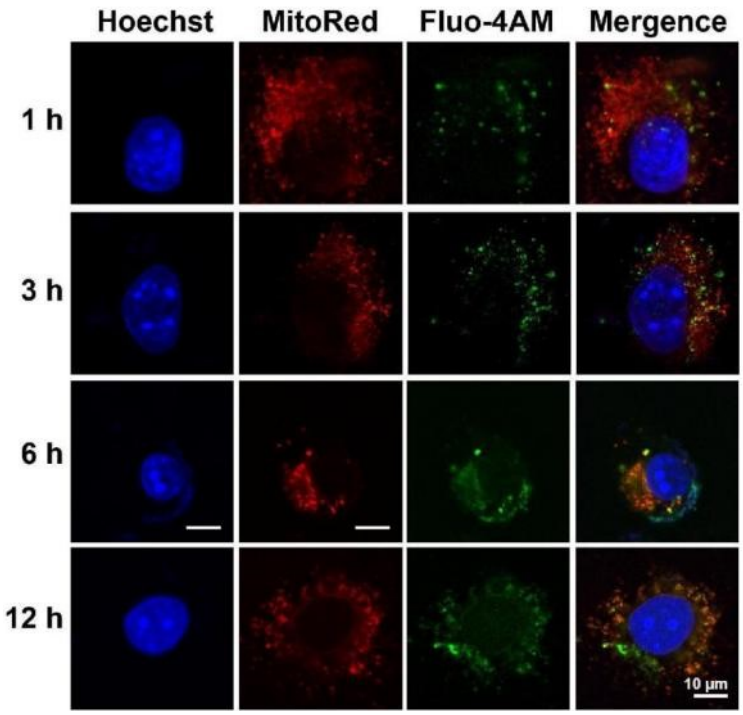

Figure S19. CLSM images (green, Fluo-4; red, MitoRed; blue, Hoechst) of distribution of Ca^{2+} in mitochondria of 4T1 cells after incubation with CaO_2@PCN for 1, 3, 6, and 12 h. Scale bar, 10 μm.

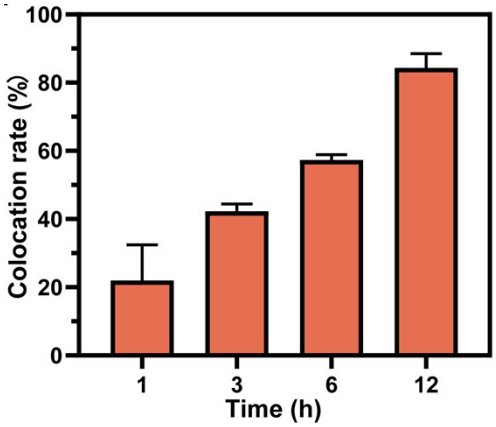

Figure S20. Colocation rate analysis of the distribution of Ca^{2+} released from CaO_2@PCN in mitochondria of 4T1 cells after incubation with CaO_2@PCN for 1, 3, 6, and 12 h. Data were expressed as mean ± SD (n = 3).

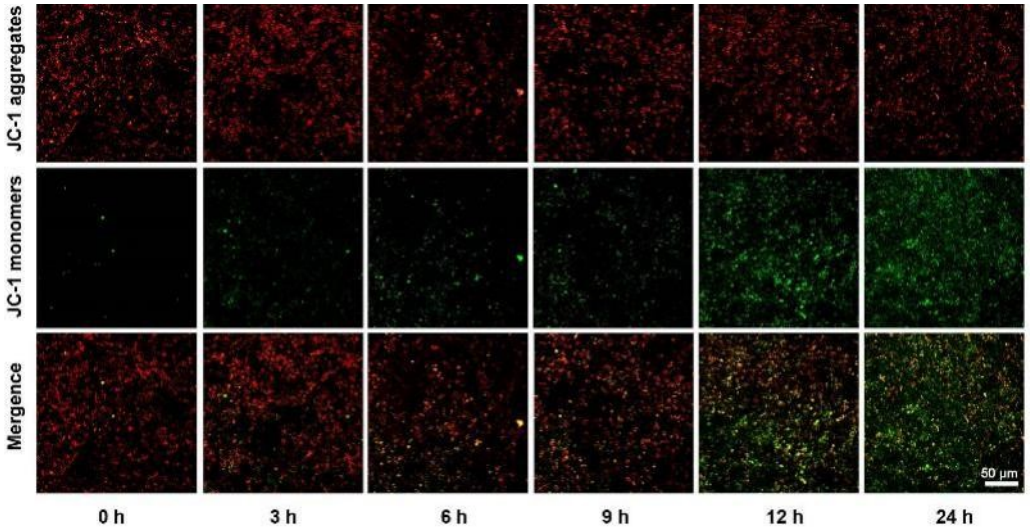

Figure S21. Fluorescent images (red, JC-1 aggregates, high membrane potential; green, JC-1 monomer, low membrane potential) of the mitochondrial membrane potential of 4T1 cells after incubation with CaO_2@PCN for 0, 3, 6, 9, 12, and 24 h. Scale bar, 50 μm.

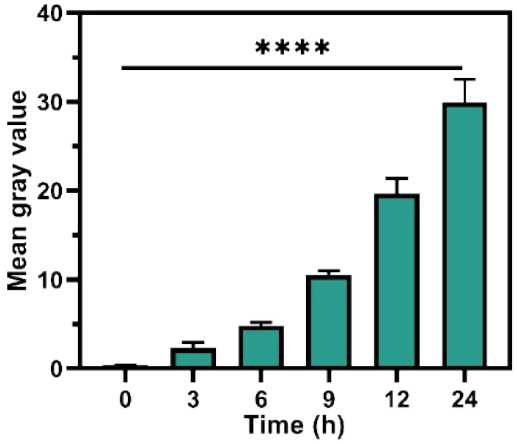

Figure S22. Quantitative analyses of mitochondrial membrane potential of 4T1 cells after incubation with CaO_2@PCN for 0, 3, 6, 9, 12, and 24 h. Data were expressed as mean ± SD (n = 3). ****P < 0.0001.

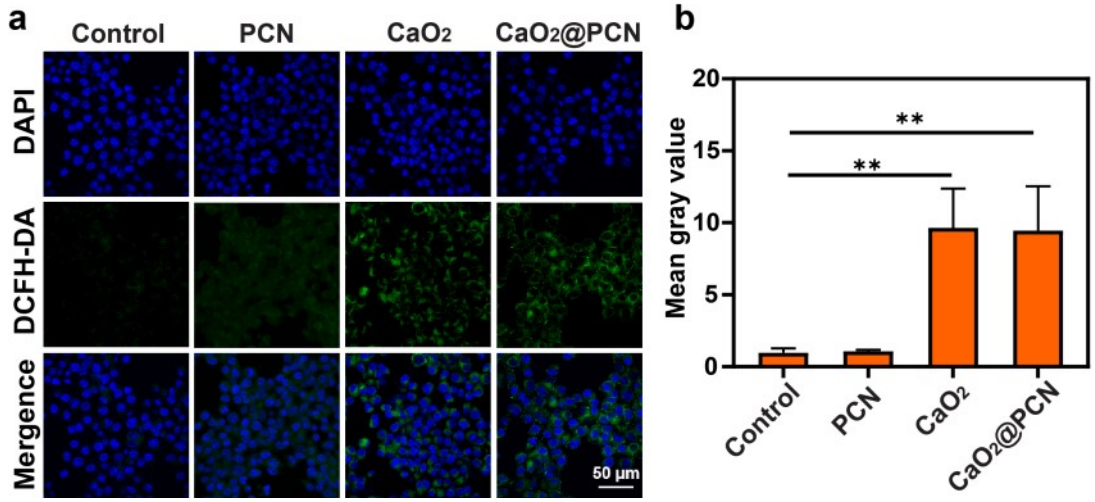

Figure S23. (a) CLSM images and (b) quantitative analyses of intracellular ROS in 4T1 cells stained with DCFH-DA (green, DCF; blue, DAPI) after different treatments. Data were expressed as mean ± SD (n = 3). **P < 0.01. Scale bar, 50 μm.

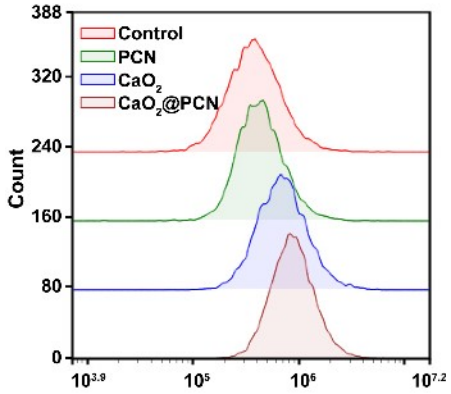

Figure S24. Flow cytometry analysis of intracellular ROS of 4T1 cells after different treatments.

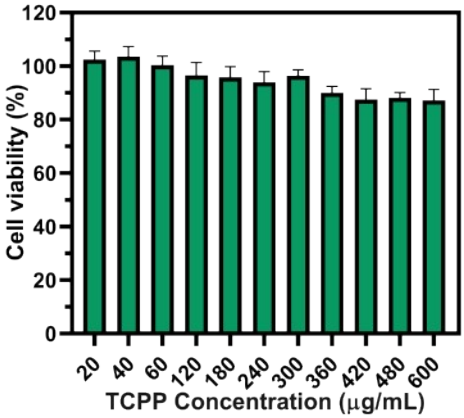

Figure S25. Relative viabilities of 4T1 cells after incubation with varied concentrations of PCN. Data were expressed as mean ± SD (n = 6).

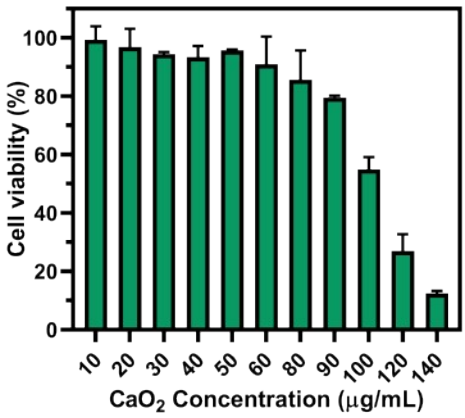

Figure S26. Relative viabilities of 4T1 cells after incubation with varied concentrations of CaO_2. Data were expressed as mean ± SD (n = 6).

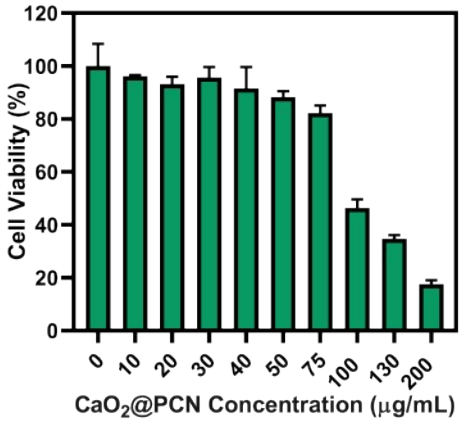

Figure S27. Relative viabilities of 4T1 cells after incubation with varied concentrations of CaO_2@PCN. Data were expressed as mean ± SD (n = 6).

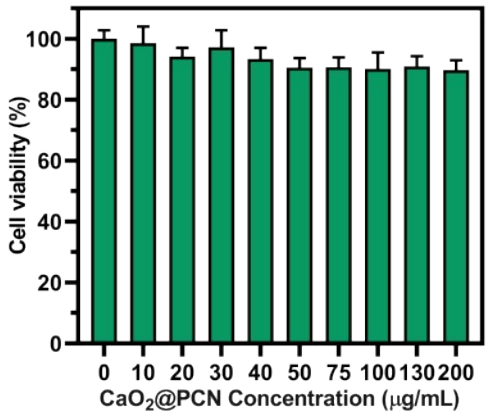

Figure S28. Relative viabilities of L929 cells after incubation with varied concentrations of CaO_2@PCN. Data were expressed as mean ± SD (n = 6).

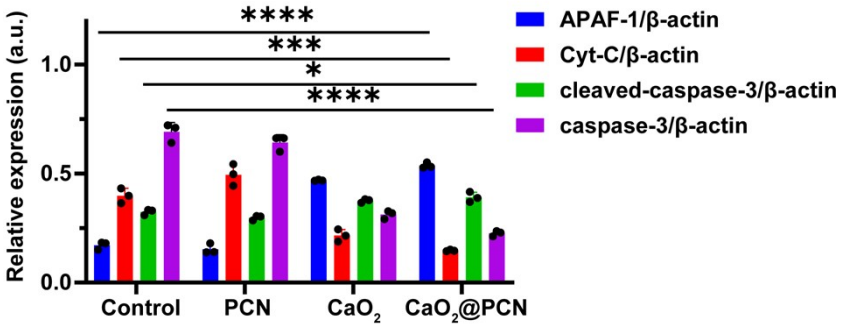

Figure S29. Quantification of western blot assay of caspase-3, cleaved-caspase-3, Cyt-C, and APAF-1 expression in 4T1 cells after various treatments. Data were expressed as mean ± SD (n = 3). **P*<0.05, ***P*<0.01, and ****P*<0.001.

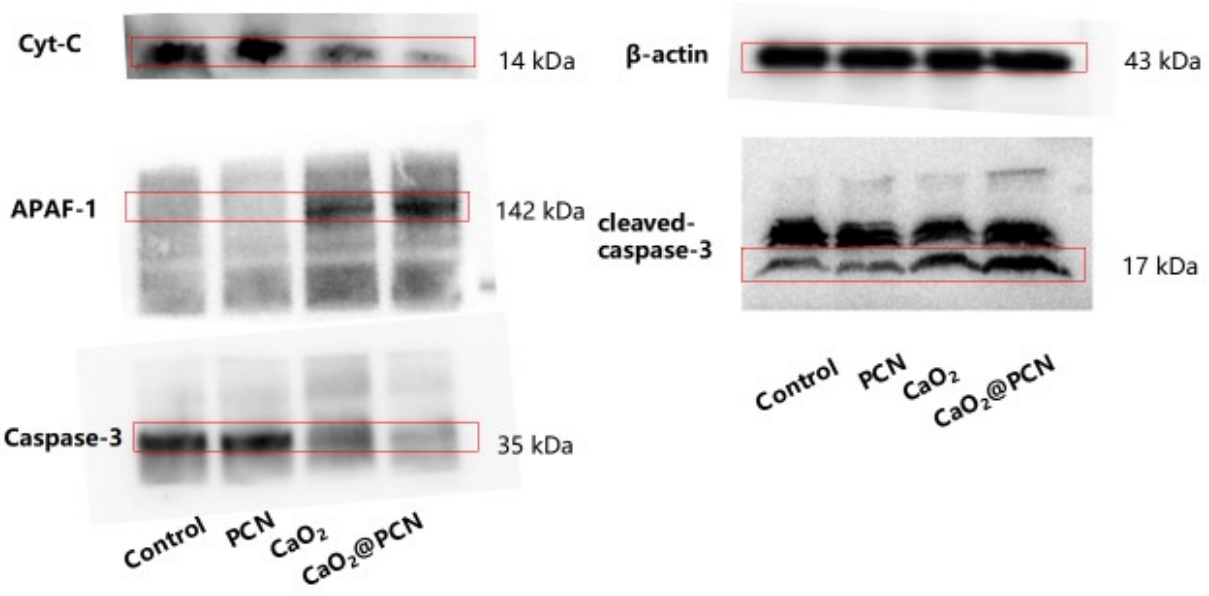

Figure S30. Uncropped strips of caspase-3, cleaved-caspase-3, Cyt-C, APAF-1, and β-actin from western-blot analysis in 4T1 cells after various treatments.

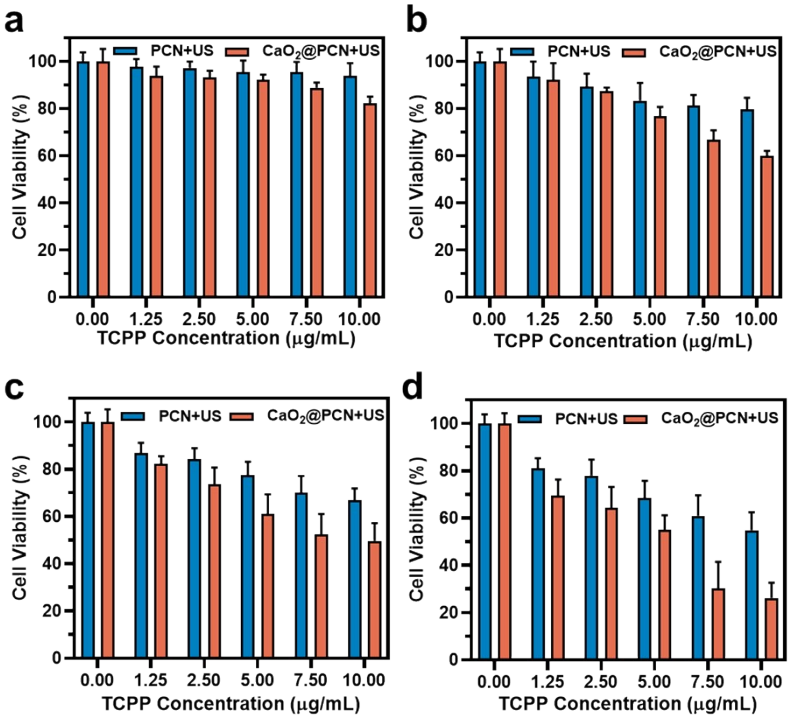

Figure S31. Relative viabilities of 4T1 cells after treatment with PCN or CaO_2@PCN with different TCPP concentrations upon varied power densities of US irradiation (a, without US; b, 1 W/cm^2; c, 1.5 W/cm^2; d, 2 W/cm^2). Data were expressed as mean ± SD (n = 6).

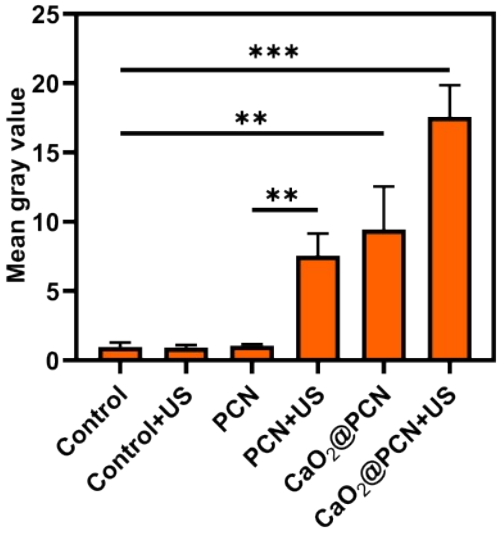

Figure S32. Quantitative analysis of intracellular ROS generation in 4T1 cells after different treatments. Data were expressed as mean ± SD (n = 3). ***P* < 0.01, ****P* < 0.001.

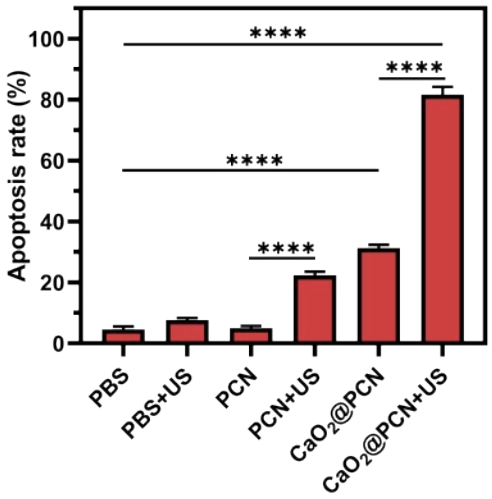

Figure S33. Quantitative analysis of apoptosis in 4T1 cells after different treatments for 24 h. Data were expressed as mean ± SD (n = 3)., *****P* < 0.0001.

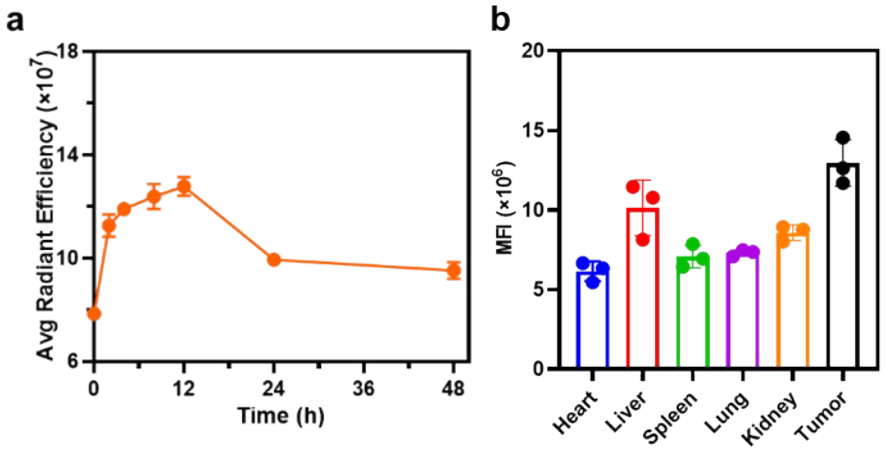

Figure S34. (a) Quantitative analysis of fluorescence intensities in tumors at given time points (0, 2, 4, 8, 12, 24, and 48 h) after i.v. injection of CaO_2@PCN. (b) Quantitative analysis of fluorescence intensities in major organs and tumors of 4T1 tumor-bearing mice at 48 h i.v. injection of CaO_2@PCN. Data were expressed as mean ± SD (n = 3).

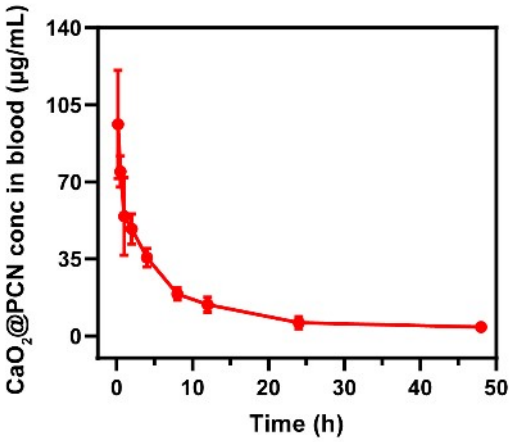

Figure S35. Blood elimination profiles of CaO_2@PCN following a single intravenous injection at a dose of 18 mg/kg in SD mice. Data were expressed as mean ± SD (n = 3).

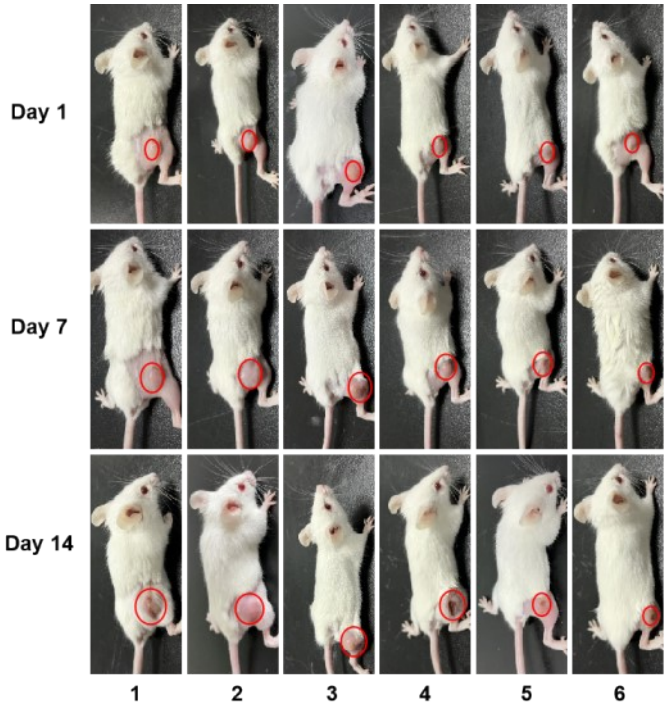

Figure S36. Photographs of 4T1 tumor-bearing mice after different treatments. 1. Control, 2. Control + US, 3. PCN, 4. PCN + US, 5. CaO_2@PCN, 6. CaO_2@PCN + US.

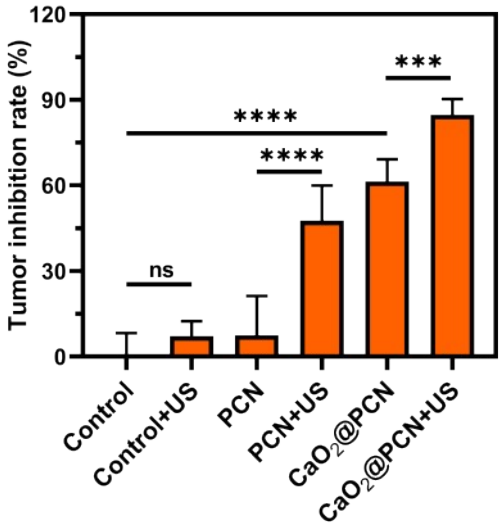

Figure S37. Specific tumor inhibition rate of 4T1 tumor-bearing mice after different treatments. Data were expressed as mean ± SD (n = 5), ***$P < 0.001$, ****$P < 0.0001$.

(The King's formula is used to calculate the q value to quantify the therapeutic effect of CaO_2@PCN + US is a synergy effect. $q = E_{(A+B)} / (E_A + E_B - E_A*E_B)$ $E_{(A+B)}$ is the tumor inhibition rate of the combination of two drugs, and E_A or E_B is the tumor inhibition rate of each drug alone. When the q value is larger than 1, it indicates that the combination of the two drugs has a synergistic effect.)

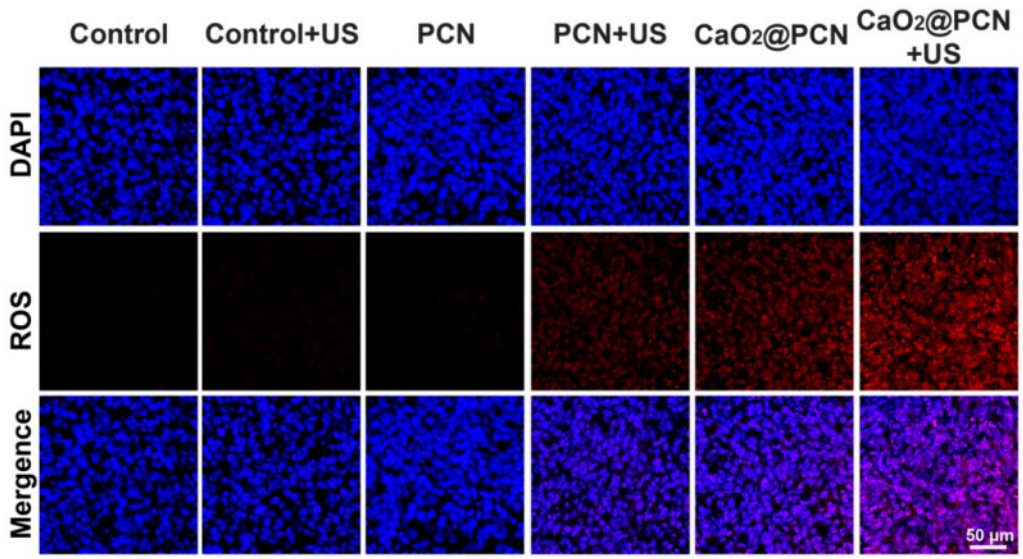

Figure S38. Immunofluorescence staining analysis of the ROS generation in 4T1 tumors after different treatments. Scale bar, 50 μm.

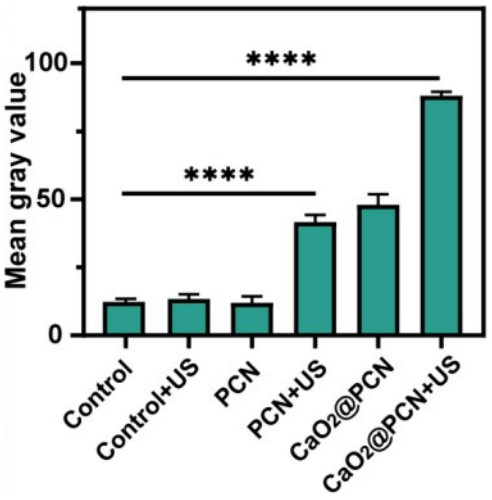

Figure S39. Quantitative analysis of the ROS generation in 4T1 tumors after different treatments. Data were expressed as mean ± SD (n = 3), ****$P < 0.0001$.

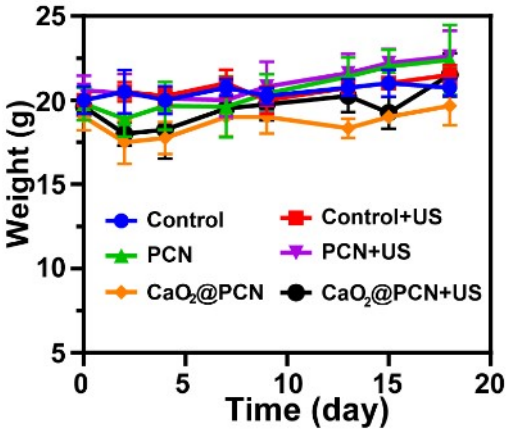

Figure S40. Body weight changes of 4T1 tumor-bearing mice after different treatments. Data were expressed as mean ± SD (n = 5).

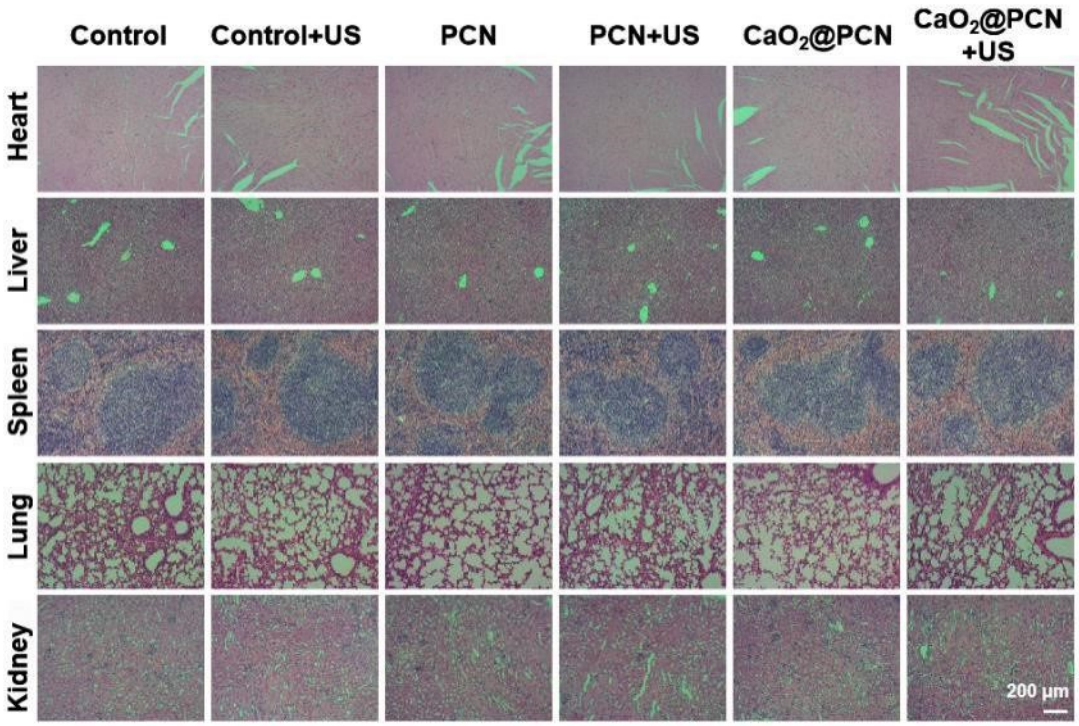

Figure S41. H&E-stained images of major organs (heart, liver, spleen, lung, kidney) harvested from 4T1 tumor-bearing mice after different treatments. Scale bar, 200 μm.

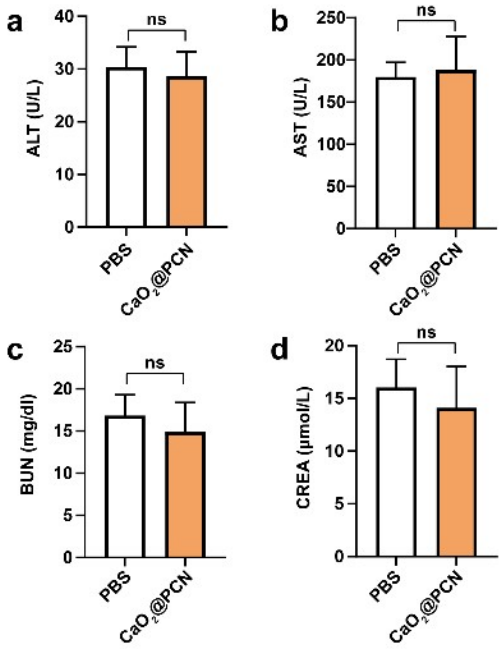

Figure S42. (a-d) Serum levels of ALT (a), AST (b), BUN (c), and CREA (d) in mice after the CaO_2@PCN treatment (n=3). Data were shown as mean ± SD. Statistical significance: **P*< 0.05, ***P* < 0.01, ****P* < 0.001, two-tailed Student's t-test.

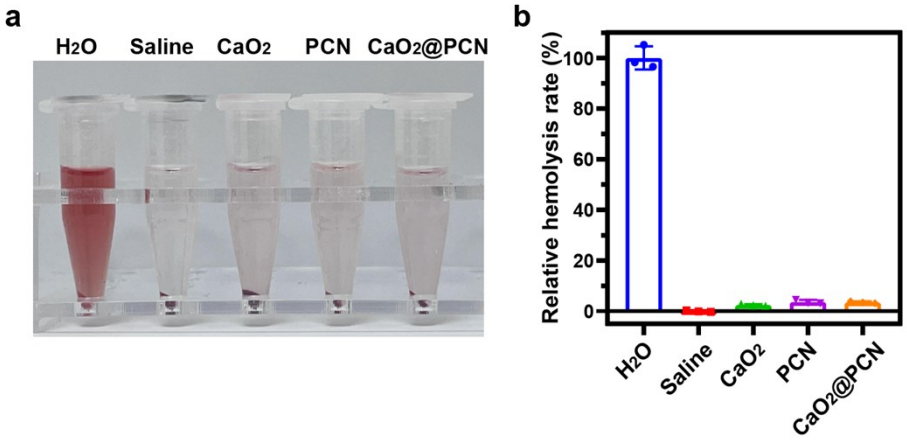

Figure S43. (a) Representative photograph and (b) relative hemolysis rate of red blood cells (RBCs) treated with different nanoparticles (CaO_2, PCN, and CaO_2@PCN), using water as a positive control and saline as a negative control. Data were expressed as mean ± SD (n = 3).